
TopoBenchmarkX: A Framework for Benchmarking Topological Deep Learning

Lev Telyatnikov
Sapienza University of Rome
lev.telyatnikov@uniroma1.it

Guillermo Bernardez
UC Santa Barbara
guillermo_bernardez@ucsb.edu

Marco Montagna
Sapienza University of Rome

Pavlo Vasylenko
Instituto Superior Técnico

Ghada Zamzmi
University of South Florida

Mustafa Hajj
University of San Francisco

Michael T. Schaub
RWTH Aachen University

Nina Miolane
UC Santa Barbara

Simone Scardapane
Sapienza University of Rome

Theodore Papamarkou
The University of Manchester

Abstract

This work introduces TopoBenchmarkX, a modular open-source library designed to standardize benchmarking and accelerate research in Topological Deep Learning (TDL). TopoBenchmarkX maps the TDL pipeline into a sequence of independent and modular components for data loading and processing, as well as model training, optimization, and evaluation. This modular organization provides flexibility for modifications and facilitates the adaptation and optimization of various TDL pipelines. A key feature of TopoBenchmarkX is that it allows for the transformation and lifting between topological domains. This enables, for example, to obtain richer data representations and more fine-grained analyses by mapping the topology and features of a graph to higher-order topological domains such as simplicial and cell complexes. The range of applicability of TopoBenchmarkX is demonstrated by benchmarking several TDL architectures for various tasks and datasets.

1 Introduction

In geometric deep learning [GDL; Bronstein et al., 2021], graph neural networks [GNNs; Zhou et al., 2020] have demonstrated impressive capabilities in processing relational data represented as graphs. However, graphs only encode pairwise structures, which can be limiting. For example, social interactions may involve multiple individuals, and electrostatic interactions in proteins may involve multiple atoms. Topological deep learning [TDL; Papamarkou et al., 2024, Bodnar, 2023, Hajj et al., 2023, Papillon et al., 2023b] offers a framework for modeling complex systems characterized by such multi-way (higher-order) relations among components. Topological neural networks [TNNs; Feng et al., 2019, Bunch et al., 2020, Hajj et al., 2020, Bodnar et al., 2021a, Ebli et al., 2020, Schaub et al., 2021, Bodnar et al., 2021b, Chien et al., 2021], which are part of TDL, have found applications in numerous fields that involve higher-order relational data such as social networks [Knoke and Yang, 2019] and protein biology [Jha et al., 2022]. TNNs achieve state-of-the-art performance in various machine learning tasks [Dong et al., 2020, Barbarossa and Sardellitti, 2020, Chen et al., 2022, Roddenberry et al., 2021, Telyatnikov et al., 2023, Giusti et al., 2023a].

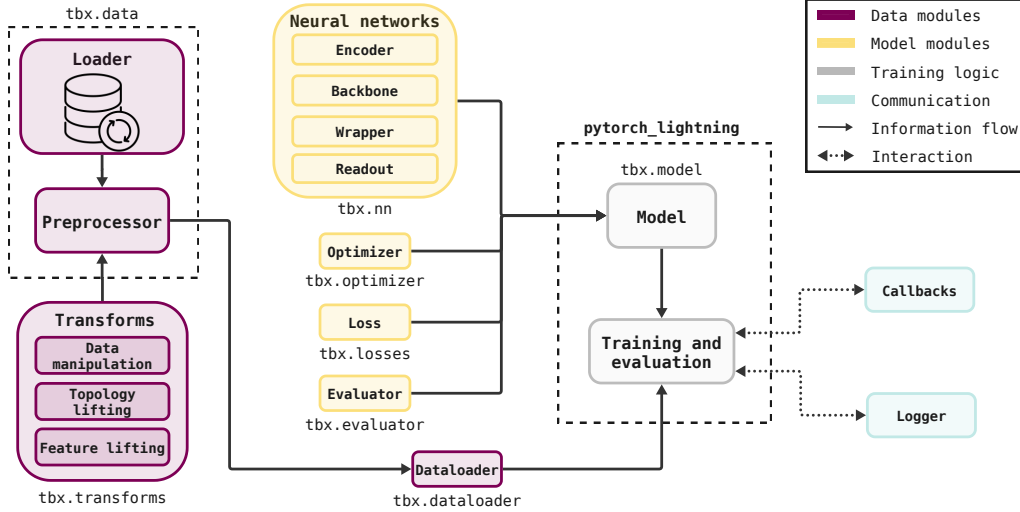


Figure 1: Workflow of TopoBenchmarkX, which consists of four main components, organized by their functionality: data modules, model modules, training modules, and communication modules.

TDL has evolved rapidly recently, providing novel algorithms for learning higher-order relational data supported on various topological domains, such as simplicial, cell, and combinatorial complexes. The works of Hajij et al. [2023] and Papillon et al. [2023b] have recently unified theory and notation of many TNNs. Moreover, the TAG ICML challenge 2023 [Papillon et al., 2023a] has contributed software implementations of topological message passing for most TNNs under TopoX [Hajij et al., 2024]. Despite these theoretical and practical advancements, the rapid acceleration of TDL research poses challenges for the reproducibility and systematic comparative evaluation of TNNs [Papamarkou et al., 2024]. In particular, open software, standardization, and benchmarking were recognized as key open challenges for TDL in a recent ICML 2024 position paper [Papamarkou et al., 2024]. TopoBenchmarkX provides a robust framework to address these issues and ensure consistent and reliable progress in the field.

TopoBenchmarkX¹ is an open-source and modular benchmarking framework for comparative evaluations of TNNs. Figure 1 visualizes the overall workflow and modularity of TopoBenchmarkX; see Section 4 for a more detailed outline. TopoBenchmarkX can generate topological datasets for benchmarking purposes, and carry out TNN comparisons based on various performance metrics. TopoBenchmarkX provides a high-level interface that reduces coding efforts, making it user-friendly. It can facilitate reproducibility of TNN research, and serves as a testbed to experiment with new ideas in TDL. Finally, TopoBenchmarkX is part of a larger suite of packages, TopoX [Hajij et al., 2024], and it is built with compatibility in mind, allowing integration with other tools and frameworks both within TopoX and in the broader PyTorch ecosystem.

Three aspects of TDL make benchmarking less straightforward: the scarcity of topological data, the non-trivial standardization of input and output across topological domains, and the diversity of TNN architectures. TopoBenchmarkX addresses these three limitations.

Generation of topological data. Although higher-order data arise in various physical systems, the complexity of capturing these interactions and the limitations of current experimental designs constrain data collection. As a result, higher-order data is often generated by lifting (i.e., transforming) graph datasets and equipping them with higher-order features. TopoBenchmarkX implements graph lifting algorithms to automate this generation process, thus mitigating the scarcity of topological datasets.

Standardization of input and output across topological domains. Each topological domain encodes higher-order relations differently. Further, each TNN architecture provides distinct mappings between inputs and outputs, and therefore processes higher-order data differently.

¹<https://github.com/pyt-team/TopoBenchmarkX>

TopoBenchmarkX standardizes the input-output pipeline through an interface that automatically manages the transition between topological domains and their associated TNNs.

Diversity of TNN architectures. There is a broad spectrum of TNNs in the TDL literature. Each TNN typically employs its own techniques to preprocess and encode data. This diversity complicates performance comparisons between models on different datasets. To address this issue, TopoBenchmarkX implements a pipeline for data preprocessing and predictive performance evaluation metrics. The pipeline is easily accessible to newcomers through a configuration file.

The rest of the paper is structured as follows. Section 2 outlines existing software for graph-based learning and benchmarking, as well as GDL. Section 3 introduces the notion of featured cell complex and formalizes the lifting of a graph to a cell complex. Section 4 introduces the main components of TopoBenchmarkX, and Section 5 demonstrates its usage via benchmarking experiments. The paper concludes with some final remarks, current limitations, and suggestions for future work in Section 6.

2 Existing software

Graph-based learning and GDL are supported by several software packages, including NetworkX [Hagberg et al., 2008], KarateClub [Rozemberczki et al., 2020], PyG [Fey and Lenssen, 2019], and DGL [Wang et al., 2019]. NetworkX enables computations on graphs, while KarateClub implements unsupervised learning algorithms for graph-structured data. PyG and DGL provide functionality for GDL as well as graph-based learning.

Various software packages implement machine learning algorithms for higher-order domains such as HyperNetX [Liu et al., 2021], XGI [Landry et al., 2023], DHG [Feng et al., 2019], and TopoX [Hajij et al., 2024]. HyperNetX facilitates computing with hypergraphs, while XGI enables computing with both hypergraphs and simplicial complexes. DHG implements deep learning algorithms for graphs and hypergraphs. TopoX is a suite of three packages: TopoNetX, TopoEmbedX, and TopoModelX, which together enable learning with TNNs. TopoNetX supports computations on graphs and higher-order domains, including simplicial complexes, cell complexes, path complexes, combinatorial complexes, and colored hypergraphs. TopoEmbedX implements algorithms to embed higher-order domains into Euclidean spaces. TopoModelX implements most of the TNNs surveyed in Papillon et al. [2023b].

The Open Graph Benchmark (OGB) is a set of datasets and a benchmark framework to facilitate reproducible graph machine learning research [Hu et al., 2020, 2021]. The OGB is applicable to graph-based learning and GDL, but not to TDL. TopoBenchmarkX aims to fill this gap by providing algorithms that generate higher-order datasets and benchmark TNNs.

3 Featured topological domains and lifting

This section extends the concept of a featured graph to featured topological domains. To make the new definitions precise, cell complexes are used as a template for other topological domains. However, all definitions provided here are applicable to other complexes implemented in TopoBenchmarkX. This section also formalizes the lifting of a featured graph to a featured topological domain. See Appendix D for an extended introduction to other higher-order domains (e.g., simplicial complexes, hypergraphs).

3.1 Featured topological domains

A featured graph is a graph equipped with functions that map nodes or edges to features Sanchez-Lengeling et al. [2021].

Definition 1 Let $\mathcal{G} = (V, E)$ be a graph, with node set V and edge set E . A featured graph is a tuple $\mathcal{G}_F = (V, E, F_V, F_E)$, where $F_V : V \rightarrow \mathbb{R}^d$ is a function that maps each node to a feature vector in \mathbb{R}^d and $F_E : E \rightarrow \mathbb{R}^k$ is a function that maps each edge to a feature vector in \mathbb{R}^k .

Definition 2 A cell complex is a triplet $\mathcal{X} = (\mathcal{X}_0, \mathcal{X}_1, \mathcal{X}_2)$ of finite ordered sets, where \mathcal{X}_0 is a set of nodes (or 0-cells), \mathcal{X}_1 is a set of edges (or 1-cells) with each edge $e \in \mathcal{X}_1$ being an ordered pair of nodes $e = [v_1, v_2]$ for $v_1, v_2 \in \mathcal{X}_0$, and \mathcal{X}_2 is a set of faces (or 2-cells) with each face $\sigma \in \mathcal{X}_2$ being an ordered sequence of edges $\sigma = [e_1, e_2, \dots, e_{m(\sigma)}]$ forming a closed path without self-intersections

and $m(\sigma) \geq 3$. A featured cell complex is a tuple $\mathcal{X}_F = (\mathcal{X}_0, \mathcal{X}_1, \mathcal{X}_2, F_{\mathcal{X}_0}, F_{\mathcal{X}_1}, F_{\mathcal{X}_2})$, where, for $0 \leq i \leq 2$, $F_{\mathcal{X}_i} : \mathcal{X}_i \rightarrow \mathbb{R}^{k_i}$ maps each cell in \mathcal{X}_i to a feature vector \mathbb{R}^{k_i} .

3.2 Liftings

In this paper, lifting refers to the process of mapping a featured graph to a featured topological domain through a well-defined procedure [Hajij et al., 2023]. We provide a precise definition for the case of cell complexes. However, lifting to other topological domains can be defined similarly.

Definition 3 Let $\mathcal{G}_F = (V, E, F_V, F_E)$ be a featured graph. A lifting of \mathcal{G}_F is a triplet $(\mathcal{C}_F, \iota, L)$, where $\mathcal{C}_F = (\mathcal{X}_0, \mathcal{X}_1, \mathcal{X}_2, F_{\mathcal{X}_0}, F_{\mathcal{X}_1}, F_{\mathcal{X}_2})$, is a featured cell complex, ι is an embedding map that maps the nodes and edges of \mathcal{G} to cells in \mathcal{X} , and L is a collection of functions that map features of \mathcal{G}_F to features of \mathcal{C}_F . The embedding map ι satisfies $\iota(v) = s_v$ for $v \in V$ with $s_v \in \mathcal{X}_0$ being a 0-cell corresponding to node v , and $\iota(e) = x_e$ for $e \in E$ with $x_e \in \mathcal{X}_1$ being a cell corresponding to edge e . The collection of functions in L consists of a lifting procedure for the higher-order cells in \mathcal{X} that are not part of \mathcal{G} and a lifting procedure for the feature maps $\{F_{\mathcal{X}_i}\}_{i=0}^2$ based on \mathcal{G}_F .

Examples of liftings are given in Figure 2. Observe that a featured cell complex in Definition 3 acts as a template for a general topological domain to which the structural and feature information of the graph is lifted. In the general case, even if the graph features are empty (that is, if F_V and F_E are not defined), lifting still provides a way to map the graph structure to the cell complex structure.

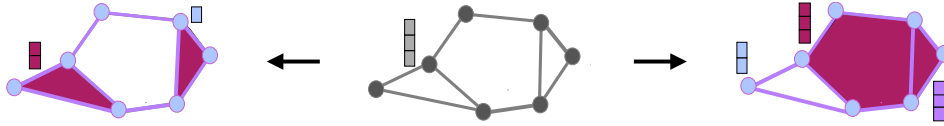


Figure 2: An illustration of lifting a featured graph \mathcal{G}_F (center) to two different topological domains: a simplicial complex (left) and a cell complex (right). The lifting from \mathcal{G}_F (center) to the featured cell complex \mathcal{C}_F (right) is represented by the triplet $(\mathcal{C}_F, \iota, L)$, where ι is the embedding map that places the nodes and edges of \mathcal{G}_F into the corresponding cells of \mathcal{C}_F , and L is the collection of functions that maps the features of \mathcal{G}_F to the features of \mathcal{C}_F .

Lifting maps can be fixed [Bodnar et al., 2021a, Hajij et al., 2023] or learnable [Battiloro et al., 2023a, Bernárdez et al., 2023]. Fixed lifting maps are predefined and follow a rule-based procedure to lift a featured graph to a featured topological domain. For example, one could define a fixed lifting that always maps a node in the graph to a node in the topological domain, and an edge to a corresponding cell. In contrast, learnable lifting maps are determined using machine learning models that are trained to optimize the lifting process based on specific criteria or objective functions. During training, the model learns to embed the nodes and edges of the input graph into the cells of a topological domain in a way that optimizes the representation for downstream tasks, such as classification or clustering. When lifting a graph to a topological domain, both the features on the higher-order cells and the structure of the topological domain itself can be computed deterministically [Ramamurthy et al., 2023] or learned [Hajij et al., 2023].²

4 Outline of TopoBenchmarkX library

TopoBenchmarkX implements a unified and flexible workflow that facilitates the addition of new datasets, transforms, and deep learning models, thus ensuring applicability across a wide range of tasks and enabling a broad cross-domain comparison, which is lacking in the TDL literature. Each module within TopoBenchmarkX is assigned a distinct role, while maintaining a consistent input-output structure, which provides a modular interface across all topological domains. Figure 1 outlines the TopoBenchmarkX modules, which are organized by functionality to data, model, training, and communication modules. Algorithm 1 exemplifies the TopoBenchmarkX execution pipeline via pseudo-code.

²An unpooling operation from lower-rank cells, where features are given, to higher-rank cells, where features are to be lifted, is called a learnable feature lifter in Hajij et al. [2023].

4.1 TopoBenchmarkX modules

Data modules. These modules include `Loader`, `Transforms`, `PreProcessor`, and `DataLoader`.

Loader. The loader module provides an interface for downloading and storing data; it includes the `GraphLoader`, `HypergraphLoader`, `SimplicialLoader`, and `CellLoader` classes. Their interfaces are built upon the widely-adopted `InMemoryDataset`, provided by PyG to enhance interoperability. The project webpage provides multiple in-depth tutorials on the library, including a step-by-step overview of incorporating customized data with these interfaces.

Transforms. *Transforms* modules are developed as sub-classes of the `BaseTransform` class provided by PyG. These modules are data manipulation, topology lifting, and feature lifting. The data manipulation module allows for performing any data transformation; e.g., the transformations available in PyG or `TopoEmbedX` can be easily adapted in `TopoBenchmarkX`. The topology lifting and feature lifting modules are responsible for lifting data from one topological domain to another. In particular, the former module relies on `TopoNetX` to lift the topology, while the latter utilizes the lifted topology to infer (e.g., project, concatenate) the features for higher-order topological structures. Each transform takes a `Data` object from PyG as input, performs the necessary computations, and outputs the modified `Data` object. The *Transforms* modules are composable operators that can be easily customized to perform various tasks.

Pre-processor. The `PreProcessor` class applies a sequence of transforms to a dataset. It takes a dataset object and a sequence of transforms as input, and iterates over the dataset, applying a set of transforms sequentially to each instance in the dataset. To avoid re-computing the same transforms multiple times, the pre-processed dataset is automatically saved in a unique folder for each transform configuration. This ensures that each dataset needs to be processed only once per configuration, addressing the potential time-consuming nature of preprocessing large datasets. `PreProcessor` also generates and/or loads data splits according to the chosen strategy; for example, random splits with predefined proportions, k-fold cross-validation, or fixed splits.

Dataloader. The `dataloader` module provides a consistent interface for batch training across all topological domains. `TopoBenchmarkX` supports mini-batching for graphs, hypergraphs, simplicial complexes, and cell complexes.

Model modules. *Neural networks* modules form the core of the modeling pipeline. The encoder module maps initial data features into a latent space and applies a learnable transformation before passing the data to the TNN model. The backbone TNN can be imported from `TopoModelX`, PyG, or it can be built on a custom basis, allowing flexibility in model selection (see Table 6 in Appendix E.2). The wrapper ensures that the correct input is provided to the forward pass of the model and collects the output in a dictionary. The wrapper plays a crucial role in the integration of any model in `TopoBenchmarkX`, making it possible to use existing and newly developed models. The readout module processes latent representations of the neural network into final output predictions. The Loss module is responsible for defining the loss function from the PyTorch library. The optimizer module defines the optimizer and scheduler. It allows for easy integration of any optimizer and scheduler from `torch.optim`, which provides flexibility in optimizing model training. The evaluator module is responsible for computing metrics during training and inference. It is built upon `torchmetrics` and supports standard metrics for classification and regression tasks.

Training and communication modules. The `Model` class defines a training pipeline for all domains (lines 14-19 of Algorithm 1). It inherits from `LightningModule`, and requires the `Encoder`, `Wrapper`, `Backbone`, `Readout`, `Evaluator`, `Loss`, and `Optimizer` objects as inputs. The `lightning.Trainer` automates the training, evaluation, and testing processes. Extra functionalities can be added using *callbacks* modules, and users can monitor the training process using different *loggers* (e.g. `wandb`, `tensorboard`). Both are common practice in `Lightning`, and they are referred to as *communication* modules in `TopoBenchmarkX`.

4.2 Topological liftings

This section explores different (structural) liftings implemented in `TopoBenchmarkX`. In particular, liftings of graphs to cell complexes, simplicial complexes, and hypergraphs are discussed.³

³Note that the modular design of `TopoBenchmarkX` easily allows for the addition of new lifting transforms between any pair of topological domains.

Algorithm 1 Execution pipeline for model training in TopoBenchmarkX

```
1: Input: General cfg configuration file
2: dataset  $\leftarrow$  Loader(cfg.dataset) # Dataset loading
3: splits  $\leftarrow$  PreProcessor(dataset, cfg.transforms) # Transforms and splits
4: dataloader  $\leftarrow$  Dataloader(dataset) # Batch generator
5: model  $\leftarrow$  Model( # Model initialization
6:   nn.Encoder(cfg.model),
7:   nn.Backbone(cfg.model),
8:   nn.BackboneWrapper(cfg.model),
9:   nn.Readout(cfg.model),
10:  *[Evaluator(cfg.evaluator), Optimizer(cfg.optimizer), Loss(cfg.loss)]
   )
11: trainer  $\leftarrow$  lightning.Trainer(cfg.trainer, cfg.callbacks, cfg.logger)

12: Model training:
13: trainer.fit(model, dataloader) # Model training

14: Model step for each batch:
15: batch  $\leftarrow$  self.encoder(batch) # Feature encoder
16: model_out  $\leftarrow$  self.forward(batch) # TNN
17: model_out  $\leftarrow$  self.readout(model_out, batch) # Readout
18: model_out  $\leftarrow$  self.loss(model_out, batch) # Loss computation
19: self.evaluator.update(model_out) # Evaluator update
```

From graphs to cell complexes: cycle-based liftings. A graph is lifted to a cell complex as follows. First, a finite set of cycles (closed loops) within the graph is identified. Second, each identified cycle in the graph is associated with a 2-cell, such that the boundary of the 2-cell is the cycle. The nodes and edges of the cell complex are inherited from the graph.

From graphs to simplicial complexes: clique complexes. By lifting a graph to a simplicial complex, both pairwise and higher-order interactions are captured. For a graph, the corresponding clique complex is formed by considering every complete subgraph (clique) as a simplex. Specifically, each node is a 0-simplex, each edge (clique of size 2) is a 1-simplex, each triangle (clique of size 3) is a 2-simplex, and so forth. In general, a clique of size $k + 1$ becomes a k -simplex.

From graphs to simplicial complexes: neighbor complexes. Neighbor complexes lift the neighborhoods of nodes to become simplices as follows. For each node in the graph, take the set of its neighbors and the node itself. These sets are then treated as simplices. The dimension of each simplex depends on the degree of the nodes. For example, a node with d neighbors forms a d -simplex.

From graphs to hypergraphs: k -hop liftings. Let $\mathcal{G} = (V, E)$ be a graph and $\mathcal{H} = (V, \mathcal{E})$ be a hypergraph. The k -neighborhood $N_k(v)$ of a node $v \in V$ in \mathcal{G} consists of all nodes reachable within k steps from v . To lift \mathcal{G} to \mathcal{H} , for each node $v \in V$, determine $N_k(v)$ and create a hyperedge e_v in \mathcal{H} such that $e_v = N_k(v)$. Thus, the set of hyperedges in \mathcal{H} is given by $\mathcal{E} = \{N_k(v) \mid v \in V\}$.

5 Numerical experiments

This section presents numerical experiments that exemplify the wide range of functionality of TopoBenchmarkX, and provide a first attempt to perform a broad cross-domain comparison. First, the general experimental setup is described. The experiments compare twelve graph, hypergraph and topological neural network models across four learning tasks related to twenty-two datasets. Subsequently, the main benchmark results are presented. Finally, it is shown how TopoBenchmarkX facilitates comparisons in TDL by conducting an ablation study for different types of signal propagation⁴.

⁴See Appendix E for an introduction to TNNs and higher-order message passing on topological domains.

5.1 Setup

Learning tasks and datasets. Four learning tasks are carried out, namely node classification (seven datasets), node regression (seven datasets), graph classification (seven datasets), and graph regression (one dataset). For node classification, cocitation datasets (Cora, Citeseer, and Pubmed), as well as heterophilic datasets (Amazon rating, Minesweeper, Roman empire, and Tolokers) are used [Platonov et al., 2023]. For node regression, the election, bachelor, birth, death, income, migration, and unemployment datasets from US election map networks are adapted [Jia and Benson, 2020]. In these datasets, nodes represent US states, edges connect neighboring states, and each state is characterized by demographic and election statistics. For each dataset, one statistic is set to be the output variable, while the remaining statistics serve as node features, referring to each such dataset with the output statistic’s name. For graph classification, the TUDataset is used, consisting of the MUTAG, PROTEINS, NCI1, NCI109, IMDB-BIN, IMDB-MUL, and REDDIT datasets; see Morris et al. [2020]. For graph regression, the ZINC dataset is employed [Irwin et al., 2012]. See Table 7 in Appendix F for descriptive summaries of the datasets.

Models. The twelve neural network models are supported on four domains: graphs, hypergraphs, simplicial complexes, and cell complexes. In particular, three GNNs (GCN, GIN, and GAT), three hypergraph neural networks (EDGNN, AllSetTransformer, and UniGNN2), three simplicial neural networks (SCN, SCCN, and SCCNN), and three cell complex neural networks (CCXN, CWN, and CCCN) are used in the experiments. Please see Appendix E.2 for further details about these architectures, including a comparison of their hyperparameter budget.

Training and evaluation. Five splits are generated for each dataset. Each split comprises 50%/25%/25% of data points in the training, validation, and test set, respectively. As an exception, the pre-defined splits for the ZINC dataset are used [Irwin et al., 2012]. The optimal hyperparameter set is selected based on the best average performance over five validation splits. See Appendix C.2 for more details on the hyperparameter search. One performance metric per dataset is reported. More specifically, the predictive accuracy is reported for Cora, Citeseer, Pubmed, Amazon, Empire, MUTAG, PROTEINS, NCI1, NCI109, IMDB-BIN, IMDB-MUL, and REDDIT; the AUC-ROC metric is reported for Minesweeper and Tolokers; the mean-squared error is reported for election, bachelor, birth, death, income, migration, and unemployment; and the mean-absolute error is reported for ZINC. For each performance metric, its mean and standard deviation are computed over the five test sets per dataset and are reported in Table 1 (note that OOM stands for ‘out of memory’ in Table 1).

5.2 Main results

As seen from Table 1, higher-order neural networks (based on hypergraphs, simplicial and cell complexes) achieve the best performance on sixteen of twenty-two datasets, whereas GNNs achieve the best performance on seven datasets. GNNs perform best on node regression in the majority of cases (five out of seven). These best results obtained by GNNs are closely matched by TNNs, since the latter attain metrics within one standard deviation from the former. In contrast, in nine out of sixteen datasets TNNs outperform GNNs, and attain performance metrics that are higher by more than one standard deviation with respect to GNNs. In other words, in the cases where higher-order networks outperform GNNs, the performance gap is more pronounced. It is also noted that, for demonstration purposes, only one fixed lifting is considered to transform graph data to each of the considered topological domains (see Appendix C.3). These results suggest that TNNs hold an advantage over GNNs, even without lifting optimization. Most importantly for the context of this paper, the benchmarks demonstrate the extent of comparisons that can be performed with TopoBenchmarkX across models and datasets.

5.3 Ablation study

Graph and hypergraph (neural network) models differ from simplicial and cell complex (neural network) models in terms of the domains and representations they support. Graph and hypergraph models can output two types of representations: node representations and edge or hyperedge representations. In contrast, the output of simplicial and cell models depends on the different types of cells present (0-cell up to n -cells) and the model itself. For example, a simplicial or cell complex

Table 1: Cross-domain comparison: results are shown as mean and standard deviation. The best result is bold and shaded in grey, while those within one standard deviation are in blue-shaded boxes.

Dataset	GCN	GIN	GAT	AST	EDGNN	UniGNN2	CWN	CCCN	SCCNN	SCN
Cora	87.09 ± 0.20	87.21 ± 1.89	86.71 ± 0.95	88.92 ± 0.44	87.06 ± 1.09	86.97 ± 0.88	86.32 ± 1.38	87.44 ± 1.28	82.19 ± 1.07	82.27 ± 1.34
Citeseer	75.53 ± 1.27	73.73 ± 1.23	74.41 ± 1.75	73.85 ± 2.21	74.93 ± 1.39	74.72 ± 1.08	75.20 ± 1.82	75.63 ± 1.58	70.23 ± 2.69	71.24 ± 1.68
Pubmed	89.40 ± 0.30	89.29 ± 0.41	89.44 ± 0.24	89.62 ± 0.25	89.04 ± 0.51	89.34 ± 0.45	88.64 ± 0.36	88.52 ± 0.44	88.18 ± 0.32	88.72 ± 0.50
Amazon	49.56 ± 0.55	49.16 ± 1.02	50.17 ± 0.59	50.50 ± 0.27	48.18 ± 0.09	49.06 ± 0.08	51.90 ± 0.15	50.26 ± 0.17	OOM	OOM
Empire	78.16 ± 0.32	79.56 ± 0.20	84.02 ± 0.51	79.50 ± 0.13	81.01 ± 0.24	77.06 ± 0.20	81.81 ± 0.62	82.14 ± 0.00	89.15 ± 0.32	88.79 ± 0.46
Minesweeper	87.52 ± 0.42	87.82 ± 0.34	89.64 ± 0.43	81.14 ± 0.05	84.52 ± 0.05	78.02 ± 0.00	88.62 ± 0.04	89.42 ± 0.00	89.0 ± 0.00	90.32 ± 0.11
Tolokers	83.02 ± 0.71	80.72 ± 1.19	84.43 ± 1.00	83.26 ± 0.10	77.53 ± 0.01	77.35 ± 0.03	OOM	OOM	OOM	OOM
Election	0.31 ± 0.02	0.28 ± 0.02	0.29 ± 0.02	0.29 ± 0.01	0.34 ± 0.02	0.37 ± 0.02	0.34 ± 0.02	0.31 ± 0.02	0.51 ± 0.03	0.46 ± 0.04
Bachelor	0.29 ± 0.02	0.31 ± 0.03	0.28 ± 0.02	0.30 ± 0.03	0.29 ± 0.02	0.31 ± 0.02	0.33 ± 0.03	0.31 ± 0.02	0.34 ± 0.03	0.32 ± 0.02
Birth	0.72 ± 0.09	0.72 ± 0.09	0.71 ± 0.09	0.71 ± 0.08	0.70 ± 0.07	0.73 ± 0.10	0.72 ± 0.09	0.71 ± 0.09	0.79 ± 0.12	0.71 ± 0.08
Death	0.51 ± 0.04	0.52 ± 0.04	0.51 ± 0.04	0.49 ± 0.05	0.52 ± 0.05	0.51 ± 0.05	0.54 ± 0.06	0.54 ± 0.06	0.55 ± 0.05	0.52 ± 0.05
Income	0.22 ± 0.03	0.21 ± 0.02	0.20 ± 0.02	0.21 ± 0.02	0.23 ± 0.02	0.23 ± 0.02	0.25 ± 0.03	0.23 ± 0.02	0.28 ± 0.03	0.25 ± 0.02
Migration	0.80 ± 0.12	0.80 ± 0.10	0.77 ± 0.13	0.78 ± 0.12	0.80 ± 0.12	0.79 ± 0.12	0.84 ± 0.13	0.84 ± 0.12	0.90 ± 0.14	0.92 ± 0.20
Unempl	0.23 ± 0.03	0.22 ± 0.02	0.23 ± 0.03	0.22 ± 0.02	0.26 ± 0.03	0.28 ± 0.02	0.25 ± 0.03	0.24 ± 0.03	0.43 ± 0.04	0.38 ± 0.04
MUTAG	69.79 ± 6.80	79.57 ± 6.13	72.77 ± 2.77	71.06 ± 6.49	80.00 ± 4.90	80.43 ± 4.09	80.43 ± 1.78	77.02 ± 9.32	76.17 ± 6.63	73.62 ± 6.13
PROTEINS	75.70 ± 2.14	75.20 ± 3.30	76.34 ± 1.66	76.63 ± 1.74	73.91 ± 4.39	75.20 ± 2.96	76.13 ± 2.70	73.33 ± 2.30	74.19 ± 2.86	75.27 ± 2.14
NCII	72.86 ± 0.69	74.26 ± 0.96	75.00 ± 0.99	75.18 ± 1.24	73.97 ± 0.82	73.02 ± 0.92	73.93 ± 1.87	76.67 ± 1.48	76.60 ± 1.75	74.49 ± 1.03
NCII09	72.20 ± 1.22	74.42 ± 0.70	73.80 ± 0.73	73.75 ± 1.09	74.93 ± 2.50	70.76 ± 1.11	73.80 ± 2.06	75.35 ± 1.50	77.12 ± 1.07	75.70 ± 1.04
IMDB-BIN	72.00 ± 2.48	70.96 ± 1.93	69.76 ± 2.65	70.32 ± 3.27	69.12 ± 2.92	71.04 ± 1.31	70.40 ± 2.02	69.12 ± 2.82	70.88 ± 2.25	70.80 ± 2.38
IMDB-MUL	49.97 ± 2.16	47.68 ± 4.21	50.13 ± 3.87	50.51 ± 2.92	49.17 ± 4.35	49.76 ± 3.55	49.71 ± 2.83	47.79 ± 3.45	48.75 ± 3.98	49.49 ± 5.08
REDDIT	76.24 ± 0.54	81.96 ± 1.36	75.68 ± 1.00	74.84 ± 2.68	83.24 ± 1.45	75.56 ± 3.19	85.52 ± 1.38	85.12 ± 1.29	77.24 ± 1.87	71.28 ± 2.06
ZINC	0.62 ± 0.01	0.57 ± 0.04	0.61 ± 0.01	0.59 ± 0.02	0.51 ± 0.01	0.60 ± 0.01	0.34 ± 0.01	0.34 ± 0.02	0.36 ± 0.02	0.53 ± 0.04

model may process an n -cell input but may not produce an n -cell output. The backbone_wrapper in TopoBenchmarkX addresses these differences in the underlying domains of the models.

There is a second difference, which is inherent in the TNNs themselves. Consider a downstream classification task. For graphs, the standard practice is to perform classification over pooled node features. However, this aspect has not been extensively studied in the TDL literature. For instance, a simplicial or cell model may update 1-cell representations (edges) or 2-cell representations (cycles or triangles) while leaving 0-cell (nodes) representations unchanged, making direct pooling over nodes potentially meaningless. One can consider more complicated update processes in which different n -cell representations are combined, which makes the notion of pooling more intricate for higher-order domains, in general. These architectural implications are complex and are related to open research questions in TDL.

However, to compare different neural network architectures, the second aforementioned difference must be addressed. To this end, the ablation study of this section considers two types of readouts to perform a rigorous evaluation: direct readout (DR), in which the downstream task is performed directly over the 0-cell representation, and signal down-propagation (SDP), in which information from higher-order cell representations is iteratively fused down to 0-cell representations using appropriate incidence matrices, followed by a linear projection over the concatenated $n - 1$ -cell signal and the fused $n - 1$ -cell representation. For instance, if a simplicial or cell complex model outputs 0-cell, 1-cell, and 2-cell representations, the signal propagates from 2-cells to 1-cells, and from 1-cells to 0-cells during readout. The downstream task is then performed over the 0-cell representations.⁵

Table 2 shows that the best-performing readout type depends on the model’s interior signal propagation. The CWN model does not update the 0-cell representation during propagation and the SDP readout strategy performs notably better, as expected. Conversely, CCCN, SCCNN, and SCN propagate information to 0-cells, so incorporating SDP readout leads to either small or minor variations in performance metrics. Please refer to Appendix C.3 for more detailed results.

These results highlight the importance of considering the structural properties of TNNs. The performance variations observed in this ablation study emphasize how critical architectural and lifting decisions are in higher-order learning models. By facilitating comparisons across a wide range of models and datasets, TopoBenchmarkX enables researchers to derive new insights and advance TDL.

6 Concluding remarks, limitations, and future work

This paper has introduced TopoBenchmarkX, an open-source benchmarking framework for TDL. TopoBenchmarkX simplifies the benchmarking process and accelerates research by organizing the TDL pipeline into a sequence of modular steps. A key feature of TopoBenchmarkX is its ability to lift between topological domains, allowing richer data representations and more detailed analyses. This capability supports the mapping of graph topology and features to higher-order topological domains,

⁵See Appendix E for an introduction to TNNs and higher-order message passing on topological domains.

Table 2: An ablation study compares the performance of CWN, CCCN, SCCNN, and SCN models on various datasets using two readout strategies, direct readout (DR) and signal down-propagation (SDP). SDP generally enhances CWN performance, whereas the effect of SDP on CCCN, SCCNN, and SCN varies based on their internal signal propagation mechanisms. Means and standard deviations of performance metrics are shown. The best results are shown in bold for each model and readout type.

Dataset	CWN		CCCN		SCCNN		SCN		
	DR	SDP	DR	SDP	DR	SDP	DR	SDP	
Node-level tasks	Cora	74.95 ± 0.98	86.32 ± 1.38	87.44 ± 1.28	87.68 ± 1.17	82.19 ± 1.07	80.65 ± 2.39	82.27 ± 1.34	79.91 ± 1.18
	Citeseer	70.49 ± 2.85	75.20 ± 1.82	75.63 ± 1.58	74.91 ± 1.25	70.23 ± 2.69	69.03 ± 2.01	71.24 ± 1.68	70.40 ± 1.53
	Pubmed	86.94 ± 0.68	88.64 ± 0.36	88.52 ± 0.44	88.67 ± 0.39	88.18 ± 0.32	87.78 ± 0.58	88.72 ± 0.50	88.62 ± 0.44
	Amazon	45.58 ± 0.25	51.90 ± 0.15	50.55 ± 0.15	50.26 ± 0.17		OOM	OOM	OOM
	Empire	66.13 ± 0.03	81.81 ± 0.62	82.14 ± 0.00	82.51 ± 0.00	89.15 ± 0.32	88.73 ± 0.12	85.89 ± 0.34	88.79 ± 0.46
	Minesweeper	48.82 ± 0.00	88.62 ± 0.04	89.42 ± 0.00	89.85 ± 0.00	87.40 ± 0.00	89.00 ± 0.00	90.32 ± 0.11	90.27 ± 0.36
	Election	0.60 ± 0.04	0.34 ± 0.02	0.31 ± 0.02	0.31 ± 0.01	0.51 ± 0.03	0.56 ± 0.04	0.46 ± 0.04	0.51 ± 0.03
	Bachelor	0.33 ± 0.03	0.33 ± 0.03	0.32 ± 0.02	0.31 ± 0.02	0.34 ± 0.03	0.34 ± 0.03	0.32 ± 0.02	0.32 ± 0.03
	Birth	0.81 ± 0.11	0.72 ± 0.09	0.71 ± 0.09	0.72 ± 0.05	0.79 ± 0.12	0.83 ± 0.12	0.71 ± 0.08	0.80 ± 0.11
	Death	0.55 ± 0.05	0.54 ± 0.06	0.54 ± 0.06	0.54 ± 0.06	0.55 ± 0.05	0.58 ± 0.05	0.52 ± 0.05	0.56 ± 0.05
	Income	0.36 ± 0.04	0.25 ± 0.03	0.23 ± 0.02	0.23 ± 0.02	0.28 ± 0.03	0.31 ± 0.03	0.25 ± 0.02	0.27 ± 0.02
	Migration	0.90 ± 0.16	0.84 ± 0.13	0.84 ± 0.10	0.84 ± 0.12	0.90 ± 0.14	0.93 ± 0.17	0.92 ± 0.20	0.96 ± 0.23
	Unempl	0.46 ± 0.04	0.25 ± 0.03	0.24 ± 0.03	0.25 ± 0.03	0.43 ± 0.04	0.45 ± 0.04	0.38 ± 0.04	0.41 ± 0.03
Graph-level tasks	MUTAG	69.68 ± 8.58	80.43 ± 1.78	80.85 ± 5.42	77.02 ± 9.32	76.17 ± 6.63	70.64 ± 3.16	71.49 ± 2.43	73.62 ± 6.13
	PROTEINS	76.13 ± 1.80	76.13 ± 2.70	73.55 ± 3.43	73.33 ± 2.30	74.19 ± 2.86	74.98 ± 1.92	75.27 ± 2.14	74.77 ± 1.69
	NCII	68.52 ± 0.51	73.93 ± 1.87	76.67 ± 1.48	77.65 ± 1.28	76.60 ± 1.75	75.60 ± 2.45	75.27 ± 1.57	74.49 ± 1.03
	NCII09	68.19 ± 0.65	73.80 ± 2.06	75.35 ± 1.50	74.83 ± 1.18	77.12 ± 1.07	75.43 ± 1.94	74.58 ± 1.29	75.70 ± 1.04
	IMDB-BIN	70.40 ± 2.02	69.28 ± 2.57	69.12 ± 2.82	69.44 ± 2.46	70.88 ± 2.25	69.28 ± 5.69	70.80 ± 2.38	68.64 ± 3.90
	IMDB-MUL	49.71 ± 2.83	49.87 ± 2.33	49.01 ± 2.63	47.79 ± 3.45	48.75 ± 3.98	46.67 ± 3.13	48.16 ± 2.89	49.49 ± 5.08
	REDDIT	76.20 ± 0.86	85.52 ± 1.38	85.12 ± 1.29	83.32 ± 0.73	75.56 ± 3.46	77.24 ± 1.87	71.28 ± 2.06	69.68 ± 4.00
	ZINC	0.70 ± 0.00	0.34 ± 0.01	0.35 ± 0.02	0.34 ± 0.02	0.36 ± 0.01	0.36 ± 0.02	0.59 ± 0.01	0.53 ± 0.04

such as simplicial and cell complexes. The effectiveness and applicability of TopoBenchmarkX has been illustrated by benchmarking several TDL architectures on many learning tasks and datasets, gaining some preliminary insights about the relative advantages of different models.

The modular and scalable properties of TopoBenchmarkX open up several opportunities for future enhancements, and simultaneously allow us to address its current limitations. One area for future work is the integration of learnable liftings, not yet implemented in the framework. This is a promising direction, since learnable liftings can learn optimal representations of topological domains for specific downstream learning tasks. A second relevant limitation is the current lack of higher-order standard datasets. Thus, a second future work direction is to incorporate higher-order datasets into TopoBenchmarkX, giving users the option to choose between downloading built-in datasets (not yet available software feature) and generating synthetic higher-order data by lifting (already available software feature). Lastly, a third critical aspect pertains to the set of performance metrics. A wider range of alternative evaluation metrics specific to TDL needs to be developed and implemented to assess expressivity, explainability, and fairness [Papamarkou et al., 2024]. More generally, users and researchers are encouraged to contribute to the development of TopoBenchmarkX in any of these three or other preferred directions.

References

- Rubén Ballester, Pablo Hernández-García, Mathilde Papillon, Claudio Battiloro, Nina Miolane, Tolga Birdal, Carles Casacuberta, Sergio Escalera, and Mustafa Hajij. Attending to topological spaces: The cellular transformer. *arXiv preprint arXiv:2405.14094*, 2024.
- Sergio Barbarossa and Stefania Sardellitti. Topological signal processing over simplicial complexes. *IEEE Transactions on Signal Processing*, 68:2992–3007, 2020.
- Claudio Battiloro, Indro Spinelli, Lev Telyatnikov, Michael Bronstein, Simone Scardapane, and Paolo Di Lorenzo. From latent graph to latent topology inference: Differentiable cell complex module. *arXiv preprint arXiv:2305.16174*, 2023a.
- Claudio Battiloro, Lucia Testa, Lorenzo Giusti, Stefania Sardellitti, Paolo Di Lorenzo, and Sergio Barbarossa. Generalized simplicial attention neural networks. *arXiv preprint arXiv:2309.02138*, 2023b.
- Guillermo Bernárdez, Lev Telyatnikov, Eduard Alarcón, Albert Cabellos-Aparicio, Pere Barlet-Ros, and Pietro Liò. Topological network traffic compression. In *Proceedings of the 2nd on Graph Neural Networking Workshop 2023*, pages 7–12, 2023.
- Cristian Bodnar. *Topological deep learning: graphs, complexes, sheaves*. PhD thesis, University of Cambridge, 2023.
- Cristian Bodnar, Fabrizio Frasca, Nina Otter, Yuguang Wang, Pietro Lio, Guido F Montufar, and Michael Bronstein. Weisfeiler and Lehman go cellular: CW networks. *Advances in Neural Information Processing Systems*, 2021a.
- Cristian Bodnar, Fabrizio Frasca, Yuguang Wang, Nina Otter, Guido F Montufar, Pietro Lio, and Michael Bronstein. Weisfeiler and Lehman go topological: Message passing simplicial networks. In *International Conference on Machine Learning*, 2021b.
- Michael M Bronstein, Joan Bruna, Taco Cohen, and Petar Veličković. Geometric deep learning: Grids, groups, graphs, geodesics, and gauges. *arXiv preprint arXiv:2104.13478*, 2021.
- Eric Bunch, Qian You, Glenn Fung, and Vikas Singh. Simplicial 2-complex convolutional neural nets. In *NeurIPS Workshop on Topological Data Analysis and Beyond*, 2020.
- Yuzhou Chen, Yulia R Gel, and H Vincent Poor. BScNets: block simplicial complex neural networks. In *Proceedings of the AAAI Conference on Artificial Intelligence*, 2022.
- Eli Chien, Chao Pan, Jianhao Peng, and Olgica Milenkovic. You are allset: a multiset function framework for hypergraph neural networks. *arXiv preprint arXiv:2106.13264*, 2021.
- Yihe Dong, Will Sawin, and Yoshua Bengio. HNHN: hypergraph networks with hyperedge neurons. In *ICML Graph Representation Learning and Beyond Workshop*, 2020.
- Stefania Ebli, Michaël Defferrard, and Gard Spreemann. Simplicial neural networks. In *NeurIPS Workshop on Topological Data Analysis and Beyond*, 2020.
- Yifan Feng, Haoxuan You, Zizhao Zhang, Rongrong Ji, and Yue Gao. Hypergraph neural networks. In *Proceedings of the AAAI Conference on Artificial Intelligence*, 2019.
- Matthias Fey and Jan E. Lenssen. Fast graph representation learning with PyTorch Geometric. In *ICLR Workshop on Representation Learning on Graphs and Manifolds*, 2019.
- Lorenzo Giusti, Claudio Battiloro, Paolo Di Lorenzo, Stefania Sardellitti, and Sergio Barbarossa. Simplicial attention neural networks. *arXiv preprint arXiv:2203.07485*, 2022.
- Lorenzo Giusti, Claudio Battiloro, Lucia Testa, Paolo Di Lorenzo, Stefania Sardellitti, and Sergio Barbarossa. Cell attention networks. In *International Joint Conference on Neural Networks*, 2023a.
- Lorenzo Giusti, Claudio Battiloro, Lucia Testa, Paolo Di Lorenzo, Stefania Sardellitti, and Sergio Barbarossa. Cell attention networks. In *International Joint Conference on Neural Networks*, 2023b.

- Aric Hagberg, Pieter Swart, and Daniel S Chult. Exploring network structure, dynamics, and function using NetworkX. Technical report, Los Alamos National Lab (LANL), Los Alamos, NM, United States, 2008.
- Mustafa Hajij, Kyle Istvan, and Ghada Zamzmi. Cell complex neural networks. In *NeurIPS Workshop on Topological Data Analysis and Beyond*, 2020.
- Mustafa Hajij, Karthikeyan Natesan Ramamurthy, Aldo Guzmán-Sáenz, and Ghada Za. High skip networks: a higher order generalization of skip connections. In *ICLR 2022 Workshop on Geometrical and Topological Representation Learning*, 2022a.
- Mustafa Hajij, Ghada Zamzmi, Theodore Papamarkou, Vasileios Maroulas, and Xuanting Cai. Simplicial complex representation learning. In *Machine Learning on Graphs (MLOG) Workshop at 15th ACM International WSDM (2022) Conference, WSDM2022-MLOG*, January 2022b.
- Mustafa Hajij, Ghada Zamzmi, Theodore Papamarkou, Nina Miolane, Aldo Guzmán-Sáenz, Karthikeyan Natesan Ramamurthy, Tolga Birdal, Tamal Dey, Soham Mukherjee, Shreyas Samaga, Neal Livesay, Robin Walters, Paul Rosen, and Michael Schaub. Topological deep learning: going beyond graph data. *arXiv preprint arXiv:1906.09068*, 2023.
- Mustafa Hajij, Mathilde Papillon, Florian Frantzen, Jens Agerberg, Ibrahim AlJabea, Ruben Ballester, Claudio Battiloro, Guillermo Bernárdez, Tolga Birdal, Aiden Brent, Peter Chin, Sergio Escalera, Simone Fiorellino, Odin Hoff Gardaa, Gurusankar Gopalakrishnan, Devendra Govil, Josef Hoppe, Maneel Reddy Karri, Jude Khouja, Manuel Lecha, Neal Livesay, Jan Meißner, Soham Mukherjee, Alexander Nikitin, Theodore Papamarkou, Jaro Prilepok, Karthikeyan Natesan Ramamurthy, Paul Rosen, Aldo Guzmán-Sáenz, Alessandro Salatiello, Shreyas N. Samaga, Simone Scardapane, Michael T. Schaub, Luca Scofano, Indro Spinelli, Lev Telyatnikov, Quang Truong, Robin Walters, Maosheng Yang, Olga Zaghen, Ghada Zamzmi, Ali Zia, and Nina Miolane. TopoX: a suite of Python packages for machine learning on topological domains. *arXiv preprint arXiv:2402.02441*, 2024.
- Weihua Hu, Matthias Fey, Marinka Zitnik, Yuxiao Dong, Hongyu Ren, Bowen Liu, Michele Catasta, and Jure Leskovec. Open graph benchmark: datasets for machine learning on graphs. In *Advances in Neural Information Processing Systems*, pages 22118–22133, 2020.
- Weihua Hu, Matthias Fey, Hongyu Ren, Maho Nakata, Yuxiao Dong, and Jure Leskovec. OGB-LSC: a large-scale challenge for machine learning on graphs. *arXiv preprint arXiv:2103.09430*, 2021.
- Jing Huang and Jie Yang. UniGNN: a unified framework for graph and hypergraph neural networks. In *Proceedings of the Thirtieth International Joint Conference on Artificial Intelligence*, 2021.
- John J Irwin, Teague Sterling, Michael M Mysinger, Erin S Bolstad, and Ryan G Coleman. ZINC: a free tool to discover chemistry for biology. *Journal of Chemical Information and Modeling*, 52(7): 1757–1768, 2012.
- Kanchan Jha, Sriparna Saha, and Hiteshi Singh. Prediction of protein–protein interaction using graph neural networks. *Scientific Reports*, 12(1):1–12, 2022.
- Junteng Jia and Austion R Benson. Residual correlation in graph neural network regression. In *ACM International Conference on Knowledge Discovery and Data Mining*, 2020.
- Thomas N Kipf and Max Welling. Semi-supervised classification with graph convolutional networks. *arXiv preprint arXiv:1609.02907*, 2016.
- David Knoke and Song Yang. *Social network analysis*. SAGE Publications, 2019.
- Nicholas W. Landry, Maxime Lucas, Iacopo Iacopini, Giovanni Petri, Alice Schwarze, Alice Patania, and Leo Torres. XGI: a Python package for higher-order interaction networks. *Journal of Open Source Software*, 8(85):5162, 2023.
- Mona Lisa and Hew Bot. My Research Software, 12 2017. URL <https://github.com/github-linguist/linguist>.

- Xu T Liu, Jesun Firoz, Andrew Lumsdaine, Cliff Joslyn, Sinan Aksoy, Brenda Praggastis, and Assefaw H Gebremedhin. Parallel algorithms for efficient computation of high-order line graphs of hypergraphs. In *International Conference on High Performance Computing, Data, and Analytics*, 2021.
- Christopher Morris, Nils M. Kriege, Franka Bause, Kristian Kersting, Petra Mutzel, and Marion Neumann. TUDataset: a collection of benchmark datasets for learning with graphs. In *ICML Workshop on Graph Representation Learning and Beyond*, 2020.
- Theodore Papamarkou, Tolga Birdal, Michael Bronstein, Gunnar Carlsson, Justin Curry, Yue Gao, Mustafa Hajij, Roland Kwitt, Pietro Liò, Paolo Di Lorenzo, et al. Position: topological deep learning is the new frontier for relational learning. *arXiv preprint arXiv:2402.08871*, 2024.
- Mathilde Papillon, Mustafa Hajij, Audun Myers, Florianand Frantzen, Ghada Zamzmi, Helen Jenne, Johan Mathe, Josef Hoppe, Michael Schaub, Theodore Papamarkou, et al. ICML 2023 topological deep learning challenge: design and results. In *Topological, Algebraic and Geometric Learning Workshop*, 2023a.
- Mathilde Papillon, Sophia Sanborn, Mustafa Hajij, and Nina Miolane. Architectures of topological deep learning: a survey on topological neural networks. *arXiv preprint arXiv:2304.10031*, 2023b.
- Oleg Platonov, Denis Kuznedelev, Michael Diskin, Artem Babenko, and Liudmila Prokhorenkova. A critical look at the evaluation of GNNs under heterophily: are we really making progress? *arXiv preprint arXiv:2302.11640*, 2023.
- Karthikeyan Natesan Ramamurthy, Aldo Guzmán-Sáenz, and Mustafa Hajij. Topo-MLP: a simplicial network without message passing. In *International Conference on Acoustics, Speech and Signal Processing*, 2023.
- T. Mitchell Roddenberry, Nicholas Glaze, and Santiago Segarra. Principled simplicial neural networks for trajectory prediction. In *International Conference on Machine Learning*, 2021.
- Benedek Rozemberczki, Oliver Kiss, and Rik Sarkar. Karate Club: an API oriented open-source Python framework for unsupervised learning on graphs. In *ACM International Conference on Information and Knowledge Management*, 2020.
- Benjamin Sanchez-Lengeling, Emily Reif, Adam Pearce, and Alexander B. Wiltschko. A gentle introduction to graph neural networks. *Distill*, 6(9):e33, 2021.
- Michael T. Schaub, Yu Zhu, Jean-Baptiste Seby, T. Mitchell Roddenberry, and Santiago Segarra. Signal processing on higher-order networks: livin’ on the edge... and beyond. *Signal Processing*, 187:108149, 2021.
- Lev Telyatnikov, Maria Sofia Bucarelli, Guillermo Bernardez, Olga Zaghen, Simone Scardapane, and Pietro Lio. Hypergraph neural networks through the lens of message passing: a common perspective to homophily and architecture design. *arXiv preprint arXiv:2310.07684*, 2023.
- Petar Veličković, Guillem Cucurull, Arantxa Casanova, Adriana Romero, Pietro Lio, and Yoshua Bengio. Graph attention networks. In *International Conference on Learning Representations*, 2018.
- Minjie Wang, Da Zheng, Zihao Ye, Quan Gan, Mufei Li, Xiang Song, Jinjing Zhou, Chao Ma, Lingfan Yu, Yu Gai, Tianjun Xiao, Tong He, George Karypis, Jinyang Li, and Zheng Zhang. Deep Graph Library: a graph-centric, highly-performant package for graph neural networks. *arXiv preprint arXiv:1909.01315*, 2019.
- Peihao Wang, Shenghao Yang, Yunyu Liu, Zhangyang Wang, and Pan Li. Equivariant hypergraph diffusion neural operators. *arXiv preprint arXiv:2207.06680*, 2022.
- Keyulu Xu, Weihua Hu, Jure Leskovec, and Stefanie Jegelka. How powerful are graph neural networks? In *International Conference on Learning Representations*, 2019.
- Omry Yadan. Hydra - a framework for elegantly configuring complex applications. Github, 2019. URL <https://github.com/facebookresearch/hydra>.

Maosheng Yang and Elvin Isufi. Convolutional learning on simplicial complexes. *arXiv preprint arXiv:2301.11163*, 2023.

Ruochen Yang, Frederic Sala, and Paul Bogdan. Efficient representation learning for higher-order data with simplicial complexes. In *Learning on Graphs Conference*, 2022.

Jie Zhou, Guanghui Cui, Shengding Hu, Zhengyan Zhang, Cheng Yang, Zhiyuan Liu, and Maosong Sun. Graph neural networks: A review of methods and applications. *AI Open*, 1:57–81, 2020.

A Societal impact and ethics

TopoBenchmarkX aims to standardize benchmarking and accelerate research in Topological Deep Learning, so we do not expect it to have any direct negative societal impact from its usage. Moreover, authors and contributors advocate for responsible use of TopoBenchmarkX, adherence to ethical guidelines, and promote transparency, fairness, and inclusivity in research.

The TopoBenchmarkX library will be constantly maintained to respect proprietary content. It will implement strict revision processes to ensure that all code implementations, libraries, and datasets have open-source licenses that guarantee their legitimate usage within the framework.

B Code availability and reproducibility

The code for TopoBenchmarkX is available on GitHub under MIT license: <https://github.com/pyt-team/TopoBenchmarkX>. The codebase adheres to best software practices, employs continuous integration, is fully documented, and provides API documentation on its website <https://pyt-team.github.io/topobenchmarkx/index.html>.

The README.md comprehensively covers all aspects of library installation and development. To replicate the experiments outlined in this work, refer to the ‘Experiments Reproducibility’ section in the README.md. Additionally, the ‘tutorials’ folder contains various tutorials showcasing the integration of new models, datasets, and transforms.

C Training details and additional results

In this section, we delve into the details of our hyperparameter search methodology, optimization strategy, computational resources utilized for conducting the experiments, and present additional results and analyses.

C.1 Experiments’ configuration and model execution

To automate the configuration of the TopoBenchmarkX modules we utilize hydra package [Yadan, 2019]. In particular, we rely on hierarchical configuration groups and registers to facilitate the easy use of the library. Specifically, there is no need to meticulously select each module to execute the pipeline in any of the domains. Simply choosing a dataset and a model automatically configures a full default pipeline, eliminating the need for manual intervention.

TopoBenchmarkX also automates the model execution and learning through the lightning library [Lisa and Bot, 2017], orchestrating the training, validation and testing processes –as well as handling any logging and callbacks.

C.2 Hyperparameter search

Five splits are generated for each dataset to ensure a fair evaluation of the models across domains. Each split comprises 50% training data, 25% validation data, and 25% test data. An exception is made for the ZINC dataset, where pre-defined splits are used [Irwin et al., 2012].

Each model in every domain has numerous specific hyperparameters that can be tuned to enhance performance. TNNs, in particular, have multiple additional parameters that can potentially improve results. To avoid the combinatorial explosion of possible hyperparameter sets, the search space is limited to the hyperparameters common across all models. The grid-search strategy is employed to find the optimal hyperparameters for each model and dataset. Specifically, the encoder hidden dimension is varied over [32, 64, 128], the encoder dropout is varied over [0.25, 0.5], the number of backbone layers is varied over [1, 2, 3, 4], the learning rate is varied over [0.01, 0.001], and the batch size is varied over [128, 256]. Additionally, for the cellular and simplicial domains, the readout type is varied over [direct readout (DR), signal down-propagation (SDP)]. If the model cannot fit into memory, the batch size, encoder hidden dimension, and number of backbone layers are decreased until the model training fits into the GPU memory.

For node-level task datasets, validation is conducted after each training epoch, continuing until either the maximum number of epochs is reached or the optimization metric fails to improve for 50 consecutive validation epochs. The minimum number of epochs is set to 50. Conversely, for graph-level tasks, validation is performed every 5 training epochs, with training halting if the performance metric does not improve on the validation set for the last 10 validation epochs. To optimize the models, `torch.optim.Adam` is combined with `torch.optim.lr_scheduler.StepLR` wherein the step size was set to 50 and the gamma value to 0.5. In total more than 100,000 runs have been performed to obtain the results. The optimal hyperparameter set is generally selected based on the best average performance over five validation splits. For the ZINC dataset, five different initialization seeds are used to obtain the average performance.

The hyperparameter search is executed on a Linux machine with 256 cores, 1TB of system memory, and 8 NVIDIA A30 GPUs, each with 24GB of GPU memory.

C.3 Results

Table 3 additionally presents the results for the CCXN and SCCN networks, which on average, perform slightly worse than the other models. As shown in Table C.3, the CCXN network performs better when using the SDP readout strategy, although the performance improvements are not as significant as those achieved by the CWN network with the same strategy. The SCCN model benefits more from utilizing the SDP readout compared to other simplicial domain models (SCN and SCCNN), showing performance improvements in 9 out of 21 cases, while SCCNN and SCN show improvements in only 3 and 5 cases, respectively. Overall, cellular models demonstrate performance enhancements on 15, 19, and 8 datasets for CCXN, CWN, and CCCN, respectively, with the SDP readout strategy. Conversely, simplicial domain models achieve 9, 3, and 5 performance improvements for SCCN, SCCNN, and SCN, respectively, with the same SDP strategy. Based on this analysis and the findings in Section 5.3, it is recommended for the new people in the TDL to opt for the SDP readout strategy if they prefer not to delve into the intricate details of interior propagation in cellular and simplicial models.

Note that for demonstration purposes, only one fixed lifting is considered for lifting graphs to each of the considered topological domains, leaving out of the scope of this paper the analysis of the optimal lifting in each particular scenario.⁶ In particular, the clique complex lifting is applied to lift the graph to a simplicial domain. Cycle-based lifting is employed to lift the graph into the cellular domain, and k -hop lifting is utilized to lift the graph into a hypergraph, where $k = 1$. Projection lifting is applied to lift the features, specifically, the features of the $n - 1$ -cell projected to the n -cell by multiplying $n - 1$ -cell representation to corresponding incidence matrices.

Table 3: Cross-domain comparison: results are shown as mean and standard deviation. The best result is bold and shaded in grey, while those within one standard deviation are in blue-shaded boxes.

	Dataset	GCN	GIN	GAT	AST	EDGNN	UniGNN2	CCXN	CWN	CCCN	SCCN	SCCNN	SCN	
Node-level tasks	Corra	87.09 ± 0.2	87.21 ± 1.89	86.71 ± 0.95	88.92 ± 0.44	87.06 ± 1.09	86.97 ± 0.88	86.79 ± 1.81	86.32 ± 1.38	87.44 ± 1.28	80.86 ± 2.16	82.19 ± 1.07	82.27 ± 1.34	
	Citeseer	75.53 ± 1.27	73.73 ± 1.23	74.41 ± 1.75	73.85 ± 2.21	74.93 ± 1.39	74.72 ± 1.08	74.67 ± 2.24	75.2 ± 1.82	75.63 ± 1.58	69.6 ± 1.83	70.23 ± 2.69	71.24 ± 1.68	
	Pubmed	89 ± 0.3	89.29 ± 0.41	89.44 ± 0.24	89.62 ± 0.25	89.04 ± 0.51	89.34 ± 0.45	88.91 ± 0.47	88.64 ± 0.36	88.52 ± 0.44	88.37 ± 0.48	88.18 ± 0.32	88.72 ± 0.5	
	Amazon	49.56 ± 0.55	49.16 ± 1.02	50.17 ± 0.59	50.5 ± 0.27	48.18 ± 0.09	49.06 ± 0.08	48.93 ± 0.14	51.9 ± 0.15	50.26 ± 0.17	OOM	OOM	OOM	
	Empire	78.16 ± 0.32	79.56 ± 0.2	84.02 ± 0.51	79.5 ± 0.13	81.01 ± 0.24	77.06 ± 0.2	81.44 ± 0.31	81.81 ± 0.62	82.14 ± 0.0	88.27 ± 0.14	89.15 ± 0.32	88.79 ± 0.46	
	Minesweeper	87.52 ± 0.42	87.82 ± 0.34	89.64 ± 0.43	81.14 ± 0.05	84.52 ± 0.05	78.02 ± 0.0	88.88 ± 0.36	88.62 ± 0.04	89.42 ± 0.0	89.07 ± 0.25	89.0 ± 0.0	90.32 ± 0.11	
	Tolokers	83.02 ± 0.71	80.72 ± 1.19	84.43 ± 1.0	83.26 ± 0.1	77.53 ± 0.01	77.35 ± 0.03	OOM	OOM	OOM	OOM	OOM	OOM	
	Election	0.31 ± 0.02	0.28 ± 0.02	0.29 ± 0.02	0.29 ± 0.01	0.34 ± 0.02	0.37 ± 0.02	0.35 ± 0.02	0.34 ± 0.02	0.31 ± 0.02	0.53 ± 0.03	0.51 ± 0.03	0.46 ± 0.04	
	Bachelor	0.29 ± 0.02	0.31 ± 0.03	0.28 ± 0.02	0.3 ± 0.03	0.29 ± 0.02	0.31 ± 0.02	0.32 ± 0.03	0.33 ± 0.03	0.31 ± 0.02	0.36 ± 0.02	0.34 ± 0.03	0.32 ± 0.02	
	Birth	0.72 ± 0.09	0.72 ± 0.09	0.71 ± 0.09	0.71 ± 0.08	0.7 ± 0.07	0.73 ± 0.11	0.74 ± 0.11	0.72 ± 0.09	0.71 ± 0.09	0.82 ± 0.09	0.79 ± 0.12	0.71 ± 0.08	
	Death	0.51 ± 0.04	0.52 ± 0.04	0.51 ± 0.04	0.49 ± 0.05	0.52 ± 0.05	0.51 ± 0.05	0.54 ± 0.06	0.54 ± 0.06	0.54 ± 0.06	0.58 ± 0.06	0.55 ± 0.05	0.52 ± 0.05	
	Income	0.22 ± 0.03	0.21 ± 0.02	0.2 ± 0.02	0.21 ± 0.02	0.23 ± 0.02	0.23 ± 0.02	0.25 ± 0.03	0.25 ± 0.03	0.23 ± 0.02	0.29 ± 0.03	0.28 ± 0.03	0.25 ± 0.02	
	Migration	0.8 ± 0.12	0.8 ± 0.1	0.77 ± 0.13	0.78 ± 0.12	0.8 ± 0.12	0.79 ± 0.12	0.85 ± 0.18	0.84 ± 0.13	0.84 ± 0.12	0.91 ± 0.18	0.9 ± 0.14	0.92 ± 0.2	
	Unempl	0.25 ± 0.03	0.22 ± 0.02	0.23 ± 0.03	0.22 ± 0.02	0.26 ± 0.03	0.28 ± 0.02	0.27 ± 0.03	0.25 ± 0.03	0.24 ± 0.03	0.43 ± 0.04	0.43 ± 0.04	0.38 ± 0.04	
	Graph-level tasks	MUTAG	69.79 ± 6.8	79.57 ± 6.13	72.77 ± 2.77	71.06 ± 6.49	80.0 ± 4.9	80.43 ± 4.09	74.89 ± 5.51	80.43 ± 1.78	77.02 ± 9.32	70.64 ± 5.9	76.17 ± 6.63	73.62 ± 6.13
		PROTEINS	75.7 ± 2.14	75.2 ± 3.3	76.34 ± 1.66	76.63 ± 1.74	73.91 ± 4.39	75.2 ± 2.96	75.63 ± 2.57	76.13 ± 2.7	73.33 ± 2.3	75.05 ± 2.76	74.19 ± 2.86	75.27 ± 2.14
		NCI1	72.86 ± 0.69	74.26 ± 0.96	75.0 ± 0.99	75.18 ± 1.24	73.97 ± 0.82	73.02 ± 0.92	74.86 ± 0.82	73.93 ± 1.87	76.67 ± 1.48	76.17 ± 1.39	76.6 ± 1.75	74.49 ± 1.03
		NCI109	72.2 ± 1.22	74.42 ± 0.7	73.8 ± 0.73	73.75 ± 1.09	74.93 ± 2.5	70.76 ± 1.11	75.66 ± 1.3	73.8 ± 2.06	75.35 ± 1.5	75.49 ± 1.39	77.12 ± 1.07	75.7 ± 1.04
		IMDB-BIN	72.0 ± 2.48	70.96 ± 1.93	69.76 ± 2.65	70.32 ± 3.27	69.12 ± 2.92	71.04 ± 1.31	70.08 ± 1.21	70.4 ± 2.02	69.12 ± 2.82	70.88 ± 3.98	70.88 ± 2.25	70.8 ± 2.38
		IMDB-MUL	49.97 ± 2.16	47.68 ± 4.21	50.13 ± 3.87	50.51 ± 2.92	49.17 ± 4.35	49.76 ± 3.35	47.63 ± 3.45	49.71 ± 2.83	47.79 ± 3.45	49.71 ± 3.7	48.75 ± 3.98	49.49 ± 5.08
		REDDIT	76.24 ± 0.54	81.96 ± 1.36	75.68 ± 1.0	74.84 ± 2.68	83.24 ± 1.45	75.56 ± 3.19	82.84 ± 2.54	85.52 ± 1.38	85.12 ± 1.29	74.44 ± 1.74	77.24 ± 1.87	71.28 ± 2.06
ZINC		0.62 ± 0.01	0.57 ± 0.04	0.61 ± 0.01	0.59 ± 0.02	0.51 ± 0.01	0.6 ± 0.01	0.4 ± 0.04	0.34 ± 0.01	0.34 ± 0.02	0.46 ± 0.08	0.36 ± 0.02	0.53 ± 0.04	

D Higher-order domains

A higher-order domain is a generalization of a graph that captures both pairwise and higher-order relationships between entities Hajij et al. [2023]. In the study of topological domains, understanding

⁶Note that learnable liftings can further optimize the predictive capacity of higher-order networks.

Table 4: An ablation study compares the performance of CCXN, CWN, CCCN, SCCN, SCCNN, and SCN models on various datasets using two readout strategies, direct readout (DR) and signal down-propagation (SDP). SDP generally enhances CWN performance, whereas the effect of SDP on CCCN, SCCNN, and SCN varies based on their internal signal propagation mechanisms. Means and standard deviations of performance metrics are shown. The best results are shown in bold for each model and readout type.

Dataset	CCXN		CWN		CCCN		SCCN		SCCNN		SCN	
	DR	SDP										
Cora	86.32 ± 1.22	86.79 ± 1.81	74.95 ± 0.98	86.32 ± 1.38	87.44 ± 1.28	87.68 ± 1.17	80.86 ± 2.16	80.06 ± 1.66	82.19 ± 1.07	80.65 ± 2.39	82.27 ± 1.34	79.91 ± 1.18
Citeseer	72.87 ± 1.13	74.67 ± 2.24	70.49 ± 2.85	75.2 ± 1.82	75.63 ± 1.58	74.91 ± 1.25	69.6 ± 1.83	68.86 ± 2.40	70.23 ± 2.69	69.03 ± 2.01	71.24 ± 1.68	70.4 ± 1.53
Pubmed	88.91 ± 0.47	88.38 ± 0.38	86.94 ± 0.68	88.64 ± 0.36	88.52 ± 0.44	88.67 ± 0.39	88.04 ± 0.51	88.37 ± 0.48	88.18 ± 0.32	87.78 ± 0.58	88.72 ± 0.5	88.62 ± 0.44
Amazon	48.93 ± 0.14	48.34 ± 0.12	45.58 ± 0.25	51.9 ± 0.15	50.55 ± 0.15	50.26 ± 0.17	OOM	OOM	OOM	OOM	OOM	OOM
Empire	80.46 ± 0.23	81.44 ± 0.31	66.13 ± 0.03	81.81 ± 0.62	82.14 ± 0.00	82.51 ± 0.0	88.2 ± 0.22	88.27 ± 0.14	89.15 ± 0.32	88.73 ± 0.12	85.89 ± 0.34	88.79 ± 0.46
Minesweeper	88.88 ± 0.36	89.76 ± 0.32	48.82 ± 0.0	88.62 ± 0.04	89.42 ± 0.00	89.85 ± 0.00	88.85 ± 0.00	89.07 ± 0.25	87.4 ± 0.0	89.0 ± 0.00	90.32 ± 0.11	90.27 ± 0.36
Election	0.39 ± 0.05	0.35 ± 0.02	0.6 ± 0.04	0.34 ± 0.02	0.31 ± 0.02	0.31 ± 0.01	0.53 ± 0.03	0.57 ± 0.02	0.51 ± 0.03	0.56 ± 0.04	0.46 ± 0.04	0.51 ± 0.03
Bachelor	0.33 ± 0.03	0.32 ± 0.03	0.33 ± 0.03	0.33 ± 0.03	0.32 ± 0.02	0.31 ± 0.02	0.36 ± 0.02	0.34 ± 0.02	0.34 ± 0.03	0.34 ± 0.03	0.32 ± 0.02	0.32 ± 0.03
Birth	0.80 ± 0.12	0.74 ± 0.11	0.81 ± 0.11	0.72 ± 0.09	0.71 ± 0.09	0.72 ± 0.05	0.82 ± 0.09	0.83 ± 0.10	0.79 ± 0.12	0.83 ± 0.12	0.71 ± 0.08	0.8 ± 0.11
Death	0.57 ± 0.06	0.54 ± 0.06	0.55 ± 0.05	0.54 ± 0.06	0.54 ± 0.06	0.54 ± 0.06	0.58 ± 0.06	0.56 ± 0.04	0.55 ± 0.05	0.58 ± 0.05	0.52 ± 0.05	0.56 ± 0.05
Income	0.25 ± 0.03	0.25 ± 0.03	0.36 ± 0.04	0.25 ± 0.03	0.23 ± 0.02	0.23 ± 0.02	0.29 ± 0.03	0.29 ± 0.03	0.28 ± 0.03	0.31 ± 0.03	0.25 ± 0.02	0.27 ± 0.02
Migration	0.80 ± 0.11	0.85 ± 0.18	0.9 ± 0.16	0.84 ± 0.13	0.84 ± 0.10	0.84 ± 0.12	0.91 ± 0.18	0.93 ± 0.17	0.90 ± 0.14	0.93 ± 0.17	0.92 ± 0.20	0.96 ± 0.23
Unempl	0.28 ± 0.05	0.27 ± 0.03	0.46 ± 0.04	0.25 ± 0.03	0.24 ± 0.03	0.25 ± 0.03	0.43 ± 0.04	0.47 ± 0.04	0.43 ± 0.04	0.45 ± 0.04	0.38 ± 0.04	0.41 ± 0.03
MUTAG	69.79 ± 4.61	74.89 ± 5.51	69.68 ± 8.58	80.43 ± 1.78	80.85 ± 5.42	77.02 ± 9.32	70.64 ± 5.90	73.62 ± 4.41	76.17 ± 6.63	70.64 ± 3.16	71.49 ± 2.43	73.62 ± 6.13
PROTEINS	75.63 ± 2.57	74.91 ± 1.85	76.13 ± 1.80	76.13 ± 2.70	73.55 ± 3.43	73.33 ± 2.30	75.05 ± 2.76	74.34 ± 3.17	74.19 ± 2.86	74.98 ± 1.92	75.27 ± 2.14	74.77 ± 1.69
NCHI	72.43 ± 1.72	74.86 ± 0.82	68.52 ± 0.51	73.93 ± 1.87	76.67 ± 1.48	77.65 ± 1.28	76.42 ± 0.88	76.17 ± 1.39	76.6 ± 1.75	75.6 ± 2.45	75.27 ± 1.57	74.49 ± 1.03
NCHI09	73.22 ± 0.48	75.66 ± 1.30	68.19 ± 0.65	73.8 ± 2.06	75.35 ± 1.50	74.83 ± 1.18	75.49 ± 1.39	75.31 ± 1.36	77.12 ± 1.07	75.43 ± 1.94	74.58 ± 1.29	75.7 ± 1.04
IMDB-BIN	70.08 ± 1.21	68.96 ± 2.03	70.4 ± 2.02	69.28 ± 2.57	69.12 ± 2.82	69.44 ± 2.46	70.88 ± 3.98	69.76 ± 3.16	70.88 ± 2.25	69.28 ± 5.69	70.8 ± 2.38	68.64 ± 3.90
IMDB-MUL	47.63 ± 3.45	48.75 ± 3.56	49.71 ± 2.83	49.87 ± 2.33	49.01 ± 2.63	47.79 ± 3.45	49.71 ± 3.70	47.31 ± 3.12	48.75 ± 3.98	46.67 ± 3.13	48.16 ± 2.89	49.49 ± 5.08
REDDIT	74.40 ± 1.50	82.84 ± 2.54	76.20 ± 0.86	85.52 ± 1.38	85.12 ± 1.29	83.32 ± 0.73	74.16 ± 1.54	74.44 ± 1.74	75.56 ± 3.46	77.24 ± 1.87	71.28 ± 2.06	69.68 ± 4.0
ZINC	0.63 ± 0.02	0.40 ± 0.04	0.70 ± 0.0	0.34 ± 0.01	0.35 ± 0.02	0.34 ± 0.02	0.55 ± 0.01	0.46 ± 0.08	0.36 ± 0.01	0.36 ± 0.02	0.59 ± 0.01	0.53 ± 0.04

Table 5: Model sizes corresponding to the best set of hyperparameters

Model	GCN	GAT	GIN	AST	EDGNN	UniGNN2	CWN	CCCN	CCXN	SCN	SCCN	SCCNN
Cora	234.63K	113.61K	105.03K	60.26K	113.29K	109.06K	343.11K	451.85K	735.37K	144.62K	155.88K	164.17K
Citeseer	525.06K	558.60K	122.05K	132.87K	258.50K	541.32K	1754.50K	1032.84K	758.41K	737.29K	782.34K	893.13K
Pubmed	114.69K	148.23K	53.38K	280.83K	147.59K	114.56K	163.72K	85.76K	277.51K	134.40K	457.99K	605.06K
MUTAG	67.97K	22.02K	38.40K	80.77K	5.73K	84.10K	334.72K	284.29K	73.86K	20.03K	398.85K	27.11K
PROTEINS	13.19K	10.11K	13.19K	14.34K	5.60K	21.31K	101.12K	34.56K	86.53K	10.24K	397.31K	26.72K
NCHI	6.72K	11.20K	154.37K	57.47K	88.19K	104.32K	124.10K	63.87K	15.87K	94.98K	131.84K	188.99K
NCHI09	23.75K	11.23K	154.50K	221.57K	88.32K	4.61K	412.29K	17.67K	71.36K	26.08K	135.75K	49.54K
IMDB-BIN	21.70K	21.83K	9.89K	114.24K	9.86K	100.61K	68.80K	19.04K	19.04K	202.63K	563.07K	285.83K
IMDB-MUL	62.08K	6.37K	18.76K	111.30K	27.01K	8.32K	19.68K	45.64K	56.26K	27.94K	545.16K	121.22K
REDDIT	13.63K	30.66K	10.08K	106.18K	5.83K	68.10K	26.66K	47.94K	57.54K	7.84K	69.31K	286.59K
Amazon	122.37K	156.16K	89.35K	155.91K	122.24K	89.22K	578.95K	310.15K	200.96K	OOM	OOM	OOM
Minesweeper	9.28K	5.89K	51.46K	118.02K	21.70K	51.33K	22.24K	35.07K	8.83K	51.97K	25.15K	33.44K
Empire	37.39K	41.81K	33.23K	257.17K	41.49K	90.90K	142.74K	86.10K	43.83K	415.89K	612.50K	240.53K
Tolokers	84.87K	151.94K	3.75K	217.99K	21.89K	13.57K	12.07K	OOM	OOM	OOM	OOM	OOM
Election	84.22K	151.30K	150.27K	217.34K	21.57K	4.58K	118.08K	234.37K	253.18K	16.64K	11.52K	415.10K
Bachelor	17.47K	151.30K	7.81K	316.93K	84.10K	3.55K	43.78K	34.88K	12.86K	27.14K	43.52K	415.10K
Birth	4.64K	30.34K	5.70K	30.21K	84.10K	13.25K	26.24K	22.40K	253.18K	103.42K	11.52K	26.98K
Death	21.63K	10.18K	7.81K	316.93K	84.10K	51.07K	26.24K	15.58K	12.86K	27.14K	11.52K	415.10K
Income	17.47K	151.30K	9.92K	217.34K	21.57K	4.58K	85.18K	12.42K	12.86K	27.14K	268.03K	105.15K
Migration	67.71K	10.18K	38.27K	80.64K	21.57K	51.07K	26.24K	15.58K	65.15K	16.64K	11.52K	415.10K
Unempl	84.22K	151.30K	117.25K	105.86K	21.57K	5.60K	101.63K	234.37K	286.46K	27.14K	11.52K	105.15K
ZINC	22.59K	22.85K	10.40K	106.82K	22.53K	102.14K	88.06K	287.74K	16.48K	24.42K	617.86K	1453.82K
Average size	75K ± 111K	89K ± 119K	54K ± 53K	150K ± 88K	59K ± 60K	74K ± 109K	210K ± 367K	170K ± 229K	158K ± 212K	107K ± 172K	263K ± 251K	313K ± 340K

Table 6: TNNs utilized in the experiments and their references

Acronym	Neural network name	Reference
Graph neural networks		
GAT	Graph attention network	Veličković et al. [2018]
GIN	Graph isomorphism network	Xu et al. [2019]
GCN	Semi-Supervised Classification with Graph Convolutional Networks	Kipf and Welling [2016]
Simplicial complexes		
SAN	Simplicial Attention Neural Networks	Giusti et al. [2022]
SCCN	Efficient Representation Learning for Higher-Order Data with Simplicial Complexes	Yang et al. [2022]
SCCNN	Convolutional Learning on Simplicial Complexes	Yang and Isufi [2023]
SCN	Simplicial Complex Neural Networks	Ebli et al. [2020]
Cellular complexes		
CAN	Cell Attention Network	Giusti et al. [2023b]
CCCN	Generalized simplicial attention neural networks ⁷	Battiloro et al. [2023b]
CXN	Cell Complex Neural Networks	Hajij et al. [2020]
CWN	Weisfeiler and Lehman Go Cellular: CW Networks	Bodnar et al. [2021a]
Hypergraphs		
AllSetTransformer	You are AllSet: A Multiset Function Framework for Hypergraph Neural Networks	Chien et al. [2021]
EDGNN	Equivariant Hypergraph Diffusion Neural Operators	Wang et al. [2022]
UniGNN	UniGNN: a Unified Framework for Graph and Hypergraph Neural Networks	Huang and Yang [2021]

the distinct properties of various higher-order domains is essential. Two key properties are set-type relations and hierarchical structures, represented by rank functions. Higher-order domains are also called topological domains.

A clarification on terminology. From a mathematical point of view, a higher-order domain is not necessarily a topological space. However, a higher-order domain consists of higher-order cells that capture information about the topology of the underlying domain. From this high-level perspective, higher-order domains (including hypergraphs) are cell structures that encode topological information. In such a context, the terms ‘higher-order domain’ and ‘topological domain’ are used interchangeably. Similarly, the terms ‘higher-order neural network’ and ‘topological neural network’ are used interchangeably.

Definition 4 (Set-type relation) *A relation in a higher-order domain is called a set-type relation if its existence is not implied by another relation in the domain.*

Set-type relations emphasize the independence of connections within a domain, allowing for a flexible representation of complex interactions.

Definition 5 (Rank function) *A rank function on a higher-order domain \mathcal{X} is an order-preserving function $rk: \mathcal{X} \rightarrow \mathbb{Z}_{\geq 0}$; i.e., $x \subseteq y$ implies $rk(x) \leq rk(y)$ for all $x, y \in \mathcal{X}$.*

Rank functions introduce a hierarchical organization, facilitating the analysis of nested relationships and enabling pooling operations in deep learning by aggregating information across different levels of the hierarchy.

Over the past few years, four topological domains have found significant applications in TDL: hypergraphs, simplicial complexes, cell complexes, and combinatorial complexes. Note that currently, TopoBenchmarkX library supports simplicial complexes, cell complexes, and hypergraphs, while the rest will be added in future work.

D.1 Hypergraphs

Definition 6 (Hypergraph) *A hypergraph \mathcal{H} on a nonempty set \mathcal{V} is a pair $(\mathcal{V}, \mathcal{E}_{\mathcal{H}})$, where $\mathcal{E}_{\mathcal{H}}$ is a non-empty subset of the powerset $\mathcal{P}(\mathcal{V}) \setminus \{\emptyset\}$ of the nodes. Elements of $\mathcal{E}_{\mathcal{H}}$ are called hyperedges.*

Hypergraphs generalize graphs by allowing edges (called hyperedges) to connect any number of nodes, representing set-type relations without hierarchical structure.

D.2 Abstract simplicial complexes

Definition 7 (Abstract simplicial complex) *An abstract simplicial complex (SC) in a non-empty set S is a pair $SC = (S, \mathcal{X})$, where \mathcal{X} is a subset of $\mathcal{P}(S) \setminus \{\emptyset\}$ such that $x \in SC$ and $y \subseteq x$ imply $y \in SC$. Elements of \mathcal{X} are called simplices.*

Simplicial complexes represent hierarchical structures where each simplex (relation) includes all its subsets, but they do not represent set-type relations independently.

D.3 Regular cell complexes

Definition 8 (Regular cell complex) *A regular cell complex is a topological space S with a partition into subspaces (cells) $\{x_{\alpha}\}_{\alpha \in P_S}$, where P_S is an index set, satisfying the following conditions:*

1. $S = \cup_{\alpha \in P_S} \text{int}(x_{\alpha})$, where $\text{int}(x)$ denotes the interior of cell x .
2. For each $\alpha \in P_S$, there exists a homeomorphism ψ_{α} , called an attaching map, from x_{α} to $\mathbb{R}^{n_{\alpha}}$ for some $n_{\alpha} \in \mathbb{N}$, called the dimension n_{α} of cell x_{α} .
3. For each cell x_{α} , the boundary ∂x_{α} is a union of finitely many cells, each having dimension less than the dimension of x_{α} .

Cell complexes provide a hierarchical interior-to-boundary structure with clear topological and geometric interpretations, but they are not based on set-type relations.

D.4 Combinatorial complexes

Definition 9 (Combinatorial complex) A combinatorial complex (CC) is a triple $(\mathcal{V}, \mathcal{X}, \text{rk})$ consisting of a set \mathcal{V} , a subset \mathcal{X} of $\mathcal{P}(\mathcal{V}) \setminus \{\emptyset\}$, and a function $\text{rk}: \mathcal{X} \rightarrow \mathbb{Z}_{\geq 0}$ with the following properties:

1. For all $v \in \mathcal{V}$, $\{v\} \in \mathcal{X}$ and $\text{rk}(v) = 0$,
2. The function rk is order-preserving, which means that if $x, y \in \mathcal{X}$ satisfy $x \subseteq y$, then $\text{rk}(x) \leq \text{rk}(y)$.

Combinatorial complexes combine hierarchical structure with set-type relations, allowing for a flexible and comprehensive representation of higher-order networks.

E Topological neural networks

Roughly speaking, a topological neural network (TNN) is a neural network that process data on a topological domain. In this section we review the basics of TNNs using the higher-order message passing paradigm introduced in Hajij et al. [2023]. All networks we experiment on in our package fall as a special case of the definition we provide here.

First, we introduce the concept of k -cochain spaces, which are essential building blocks for topological neural networks.

Definition 10 (k-cochain spaces) Let $\mathcal{C}^k(\mathcal{X}, \mathbb{R}^d)$ be the \mathbb{R} -vector space of functions $\mathbf{H}_k: \mathcal{X}^k \rightarrow \mathbb{R}^d$ for a rank $k \in \mathbb{Z}_{\geq 0}$ and dimension d . d is called the **data dimension**. $\mathcal{C}^k(\mathcal{X}, \mathbb{R}^d)$ is called the **k -cochain space**. Elements \mathbf{H}_k in $\mathcal{C}^k(\mathcal{X}, \mathbb{R}^d)$ are called **k -cochains** or **k -signals**.

Cochain represent the input topological data (feature vectors) defined on the topological domain. To describe how data is exchanged within a topological domain, we recall the concept of neighborhood functions.

Definition 11 (Neighborhood function) Let S be a nonempty set. A **neighborhood function** on S is a function $\mathcal{N}: S \rightarrow \mathcal{P}(\mathcal{P}(S))$ that assigns to each point x in S a nonempty collection $\mathcal{N}(x)$ of subsets of S . The elements of $\mathcal{N}(x)$ are called **neighborhoods** of x with respect to \mathcal{N} .

Definition 12 (TNN) Let \mathcal{X} be a topological domain. Let $\mathcal{C}^{i_1} \times \mathcal{C}^{i_2} \times \dots \times \mathcal{C}^{i_m}$ and $\mathcal{C}^{j_1} \times \mathcal{C}^{j_2} \times \dots \times \mathcal{C}^{j_n}$ be a Cartesian product of m and n cochain spaces defined on \mathcal{X} . A **topological neural network (TNN)** is a function of the form

$$TNN: \mathcal{C}^{i_1} \times \mathcal{C}^{i_2} \times \dots \times \mathcal{C}^{i_m} \longrightarrow \mathcal{C}^{j_1} \times \mathcal{C}^{j_2} \times \dots \times \mathcal{C}^{j_n}.$$

A TNN takes as input a vector of cochains $(\mathbf{H}_{i_1}, \dots, \mathbf{H}_{i_m})$ and produces as output a vector of cochains $(\mathbf{K}_{j_1}, \dots, \mathbf{K}_{j_n})$. This framework allows for the processing of complex topological data through neural network operations.

Finally, we introduce the concept of higher-order message passing, which is the mechanism by which TNNs can exchange information across different cells in the topological domain:

E.1 Higher-order message passing

Higher-order message passing refers to a computational framework that involves exchanging messages among entities and cells in a higher-order domain using a set of neighborhood functions.

Definition 13 (Higher-order message passing on a topological domain) Let \mathcal{X} be a topological domain, and let $\mathcal{N} = \{\mathcal{N}_1, \dots, \mathcal{N}_n\}$ be a set of neighborhood functions defined on \mathcal{X} . Consider a cell x and another cell $y \in \mathcal{N}_k(x)$ for some $\mathcal{N}_k \in \mathcal{N}$. A **message** $m_{x,y}$ between cells x and y is a computation depending on these two cells or on the data they support. Let $\mathcal{N}(x)$ denote the multi-set $\{\{\mathcal{N}_1(x), \dots, \mathcal{N}_n(x)\}\}$, and let $\mathbf{h}_x^{(l)}$ represent the data supported on the cell x at layer l .

Higher-order message passing on \mathcal{X} , induced by \mathcal{N} , is defined through the following update rules:

$$m_{x,y} = \alpha_{\mathcal{N}_k}(\mathbf{h}_x^{(l)}, \mathbf{h}_y^{(l)}), \quad (1)$$

$$m_x^k = \bigoplus_{y \in \mathcal{N}_k(x)} m_{x,y}, \quad 1 \leq k \leq n, \quad (2)$$

$$m_x = \bigotimes_{\mathcal{N}_k \in \mathcal{N}} m_x^k, \quad (3)$$

$$\mathbf{h}_x^{(l+1)} = \beta(\mathbf{h}_x^{(l)}, m_x). \quad (4)$$

Here, \bigoplus is a permutation-invariant aggregation function called the **intra-neighborhood** aggregation of x , and \bigotimes is an aggregation function called the **inter-neighborhood** aggregation of x . The functions $\alpha_{\mathcal{N}_k}$ and β are differentiable functions.

To summarize:

- $m_{x,y}$ is the message computed from x to y using the function $\alpha_{\mathcal{N}_k}$.
- m_x^k aggregates all messages from the neighbors y in the neighborhood $\mathcal{N}_k(x)$ using the intra-neighborhood function \bigoplus .
- m_x further aggregates these results across all neighborhoods $\mathcal{N}_k \in \mathcal{N}$ using the inter-neighborhood function \bigotimes .
- $\mathbf{h}_x^{(l+1)}$ updates the data on cell x by combining its current data $\mathbf{h}_x^{(l)}$ with the aggregated message m_x using the function β .

E.2 Information about neural network models

In this section, we review the architectures of topological neural networks (TNNs) applied to hypergraphs, simplicial complexes, and cellular complexes; for a more comprehensive survey on TNN architectures, refer to Papillon et al. [2023b].

E.2.1 Hypergraphs neural networks

Hypergraph neural networks (HGNNs) have been extensively researched and surveyed. Early methods often reduced hypergraphs to graphs using algorithms such as clique-expansion, which compromised performance by losing structural information Dong et al. [2020]. Current models preserve hypergraph structures and typically employ a two-phase message-passing scheme, transferring information from nodes to hyperedges and then back to nodes.

Standard message passing. Models such as HyperSage, HGNN, Dynamic Hypergraph Neural Network, and UniGCN use standard message passing Wang et al. [2019], Liu et al. [2021], Huang and Yang [2021], Chien et al. [2021]. Notably, some models like UniGCN incorporate fixed weight matrices on top of learnable weights. Other approaches, such as AllSet and EHNN, enhance expressiveness using multi-set functions and sparse symmetric tensors, respectively Chien et al. [2021], Wang et al. [2022].

Attention-based message passing. Models like Dynamic Hypergraph Convolutional Network (SAN), Less is More: Hypergraph Attention Network (SAT), and UniGAT integrate attention mechanisms into the two-phase scheme. Transformer-based variants and multi-head attention are also employed to further enhance performance Wang et al. [2019], Liu et al. [2021].

E.2.2 Simplicial complexes neural networks

Initial research on simplicial complexes focused on signal processing. HodgeNet was one of the first models to learn convolutions on edge features, while subsequent models like SNN and SCCONV generalized convolutions to higher-order features Bodnar et al. [2021a], Bunch et al. [2020], Yang and Isufi [2023].

Standard message passing. Simplicial neural networks (SNNs), SCCONV, and more recent models utilize various neighborhood schemes to enhance message passing flexibility Giusti et al. [2022],

Ebli et al. [2020]. High Skip Networks (HSNs) introduce higher-order skip-connections to propagate features through multiple ranks Hajij et al. [2022a].

Attention-based message passing. Models such as SAN, SAT, and SGAT leverage attention mechanisms on simplicial domains, each utilizing unique neighborhood structures and attention coefficients Giusti et al. [2022], Hajij et al. [2022b], Battiloro et al. [2023b].

E.2.3 Cellular complexes neural networks

Building on signal processing advancements, Cell Complex Neural Networks (CXNs) Hajij et al. [2020] were introduced theoretically and later implemented in (CWN) Bodnar et al. [2021a]. The only attention-based cellular network that is Cell Attention Networks (CAN) introduced in Giusti et al. [2023b]. Recently, a cellular transformer architecture (CT) was introduced in Ballester et al. [2024].

F Descriptive summaries of datasets

Table 7 provides the statistics for each dataset lifted to three topological domains: simplicial complex, cellular complex, and hypergraph. The 0-cell, 1-cell, 2-cell, and 3-cell represents the count of n -cell each dataset have after the topology lifting procedure. The clique complex lifting is applied to lift the graph to a simplicial domain with a maximum n equal to three. Cycle-based lifting is employed to lift the graph into the cellular domain (maximum n is equal to two), and k -hop lifting is utilized to lift the graph into a hypergraph, where $k = 1$.

Table 7: Descriptive summaries of the datasets used in the experiments.

Dataset	Domain	0-cell	1-cell	2-cell	3-cell	Num. Hyperedges
Cora	Cellular	2708	5278	2648	0	0
	Simplicial	2708	5278	1630	220	0
	Hypergraph	2708	0	0	0	2708
Citeseer	Cellular	3327	4552	1663	0	0
	Simplicial	3327	4552	1167	255	0
	Hypergraph	3327	0	0	0	3327
PubMed	Cellular	19717	44324	23605	0	0
	Simplicial	19717	44324	12520	3275	0
	Hypergraph	19717	0	0	0	19717
MUTAG	Cellular	3371	3721	538	0	0
	Simplicial	3371	3721	0	0	0
	Hypergraph	3371	0	0	0	3371
NCII	Cellular	122747	132753	14885	0	0
	Simplicial	122747	132753	186	0	0
	Hypergraph	122747	0	0	0	122747
NCII109	Cellular	122494	132604	15042	0	0
	Simplicial	122494	132604	183	0	0
	Hypergraph	122494	0	0	0	122494
PROTEINS	Cellular	43471	81044	38773	0	0
	Simplicial	43471	81044	30501	3502	0
	Hypergraph	43471	0	0	0	43471
REDDIT-BINARY	Cellular	859254	995508	141218	0	0
	Simplicial	859254	995508	49670	1303	0
	Hypergraph	859254	0	0	0	859254
IMDB-BINARY	Cellular	19773	96531	77758	0	0
	Simplicial	19773	96531	391991	1694513	0
	Hypergraph	19773	0	0	0	19773
IMDB-MULTI	Cellular	19502	98903	80901	0	0
	Simplicial	19502	98903	458850	2343676	0
	Hypergraph	19502	0	0	0	19502
ZINC	Cellular	277864	298985	33121	0	0
	Simplicial	277864	298985	769	0	0
	Hypergraph	277864	0	0	0	277864
Amazon Ratings	Cellular	24492	93050	68553	0	0
	Simplicial	24492	93050	110765	64195	0
	Hypergraph	24492	0	0	0	24492
Minesweeper	Cellular	10000	39402	28955	0	0
	Simplicial	10000	39402	39204	9801	0
	Hypergraph	10000	0	0	0	10000
Roman Empire	Cellular	22662	32927	10266	0	0
	Simplicial	22662	32927	7168	0	0
	Hypergraph	22662	0	0	0	22662
Tolokers	Cellular	OOM	OOM	OOM	OOM	OOM
	Simplicial	OOM	OOM	OOM	OOM	OOM
	Hypergraph	11758	0	0	0	11758
US-county-demos	Cellular	3224	9483	6266	0	0
	Simplicial	3224	9483	6490	225	0
	Hypergraph	3224	0	0	0	3224